JOURNAL OF MATERIALS SCIENCE 26 (1991) 6800–6808

Strengthening and toughening of cordierite by the addition of silicon carbide whiskers, platelets and particles

I. WADSWORTH, R. STEVENS
Division of Ceramics, School of Materials, University of Leeds, Leeds LS2 9JT, UK

Cordierite containing silicon carbide of different morphologies has been fabricated to produce composites with superior properties to the unreinforced cordierite. It has been demonstrated that the morphology of the silicon carbide affects the densification and the mechanical properties of the composites they constitute. The densification process was controlled by the degree of mutual contact of the silicon carbide phase within the cordierite matrix and by the rigidity of the resulting networks. The operative toughening mechanisms and their relative contributions were also dependent on the morphology of the silicon carbide. Fracture strength of the composites was governed by the relative contributions of an improvement in fracture toughness and by the magnitude of the critical flaw size.

1. Introduction

Silicon carbide whiskers have been incorporated into numerous ceramic matrices in attempts to improve their mechanical properties, in particular their resistance to catastrophic failure. The majority of published data has indicated that this can be achieved. However, two potential drawbacks to the use of whiskers have been identified. Firstly, their presence has a detrimental effect on the densification processes and secondly, they have been shown to be a potential health hazard [1–3].

Direct comparisons have been made between selected mechanical properties of cordierite composites containing silicon carbide whiskers, silicon carbide powder and silicon carbide platelets to attempt to determine the operative toughening mechanisms and to explain the variations in fracture strength.

2. Experimental procedure

Cordierite SAM 194 CR was utilized as the matrix material throughout this study. The pertinent dimensional data obtained from the batch of whiskers provided is presented in Table I. The median particle size of the silicon carbide powder, as determined by sedigraph analysis, was 1 μm; 100 % of the population had an equivalent spherical diameter of less than 6 μm. The platelets have been sized to − 325 mesh (< 50 μm), but have diameters ranging from 10–70 μm and thickness ranging from 5–20 μm.

It is well established that silicon carbide whiskers may contain surface impurities such as amorphous silica and traces of metallic elements [4, 5]. In order to remove these, the whiskers were exposed to an aqueous solution of 10 % HCl and 10 % HF for 24 h. Repeated washing with distilled water took place until the effluent had a neutral pH. The whiskers were then dried over a hot plate. The same procedure was adopted for the silicon carbide powder and silicon carbide platelets to ensure consistency of surface composition. Dispersion of the whiskers and particulate silicon carbide in the cordierite powder was accomplished by mixing the appropriate masses of each constituent in distilled water, de-agglomerating using an ultrasonic probe and tumble mixing for 24 h. Dispersion of the much larger platelets was accomplished by rotary-mixing water-based suspensions for 24 h. All suspensions were rapidly frozen in liquid-nitrogen-chilled vessels and freeze dried. The composite powders were consolidated by uniaxially hot pressing in an induction-heated graphite die.

The fracture toughness of the composites was evaluated using the indentation technique [6–8]. Ten indentations per specimen were made on polished sections prepared in the plane perpendicular to the hot-pressing axis. The fracture strengths of the composites were determined by testing eight bars per specimen in four-point bending (outer span 20 mm, inner span 6 mm). The dimensions of each bar, measured to two decimal places, were approximately 4 mm × 3 mm × 22 mm. The tensile faces of the specimens were polished to a 6 μm finish and the edges of the faces were bevelled and polished to remove any machining damage.

3. Results and discussion

3.1. Consolidation of composites

In order to densify the composites, more severe conditions were required than for the unreinforced cordierite. The conditions required were dependent on both the volume fraction of the second phase present and its morphology. Table II illustrates how the different morphologies of the silicon carbide affected the densification process.

It is suggested that three possible mechanisms should be considered responsible for retarding densification.

(i) The cordierite powder contained significant amounts of an amorphous phase (Fig. 1). At elevated temperatures the presence of all silicon carbide will increase the resistance of the system as a whole to plastic flow by reducing the effect of the amorphous phase.

(ii) Second phases will produce back stresses in the matrix phase which, in turn, reduce the driving force for, and thus the rate of, densification [9].

(iii) The formation of contiguous networks of the second phase will oppose the densification process in a similar manner to that described above.

The reduction in the effective volume fraction of amorphous phase is dependent on the volume fraction of silicon carbide added. Thus the differences highlighted in Table II may not be explained using this argument. This high aspect ratio of the silicon carbide whiskers would be expected to lead to the formation of contiguous networks at volume fractions below that required for the particulate silicon carbide. Moreover, greater pressures are required to bring about their collapse, further hindering densification.

The relative ease in densifying those composites containing silicon carbide platelets compared to the other composites was attributed to their large dimensions rather than to morphological differences. Such was their average size, that mutual contact was rare; even at concentrations of 30 vol % (Fig. 2).

3.2. Fracture toughness

The fracture toughness data for the various compositions are presented in Fig. 3 and Table III. Fracture toughness was improved with increasing second phase content, regardless of its morphology, although clear differences in effectiveness were apparent.

The introduction of 30 vol % whiskers increased the fracture toughness by 78%, compared to the unreinforced cordierite. Their presence transformed the fracture surfaces from a relatively flat topography, characteristic of an unimpeded crack front, to irregular, due to extensive crack front perturbations. Such perturbations are indicative of extensive interaction of the crack front with the whiskers.

Studies of fracture surfaces and indentation-generated cracks on relief polished surfaces in the scanning

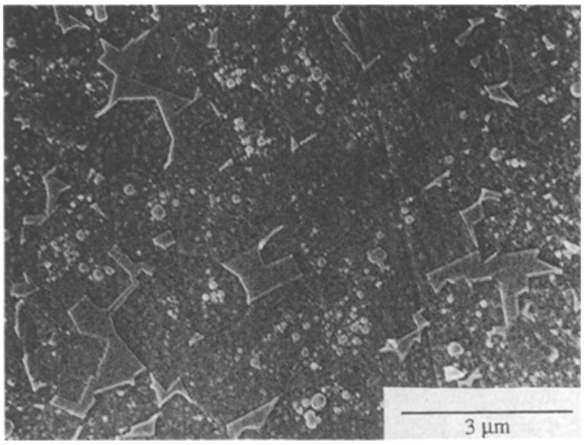

Figure 1 Scanning electron micrograph of a polished and etched surface of the hot-pressed cordierite, illustrating the presence of significant amounts of an amorphous phase. Etching conditions were 10 s in 1% HF.

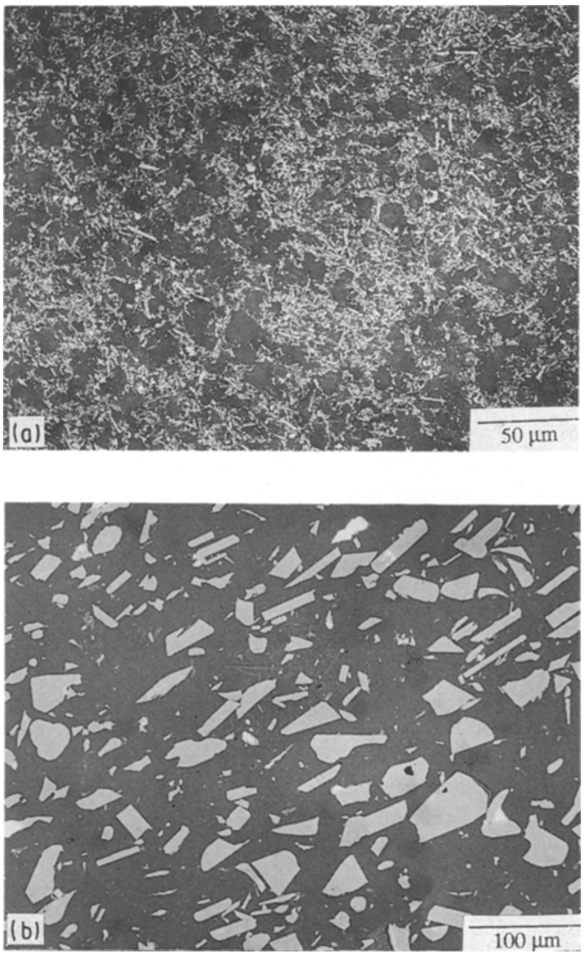

Figure 2 Optical micrographs of cordierite composites containing (a) 30 vol % SiC whiskers, and (b) 30 vol % SiC platelets. Note the differences in mean spacing due to the differences in morphology and dimensions of the second phase.

TABLE I Dimensional data representing the batch of whiskers used in this study

	Length, l (μm)	Diameter, d (μm)	Aspect ratio ($s = l/d$)
Mean	16.8	0.67	24.2
S.D.	8.5	0.22	11.9

TABLE II The hot-pressing conditions used to densify cordierite containing 30 vol % silicon carbide of different morphologies

Morphology of the SiC	Pressure (MPa)	Time (min)	Temp. (°C)	Density (% theoretical)
Whisker	25	45	145	98.3
Powder	25	20	1425	99.3
Platelet	20	20	1400	99.8

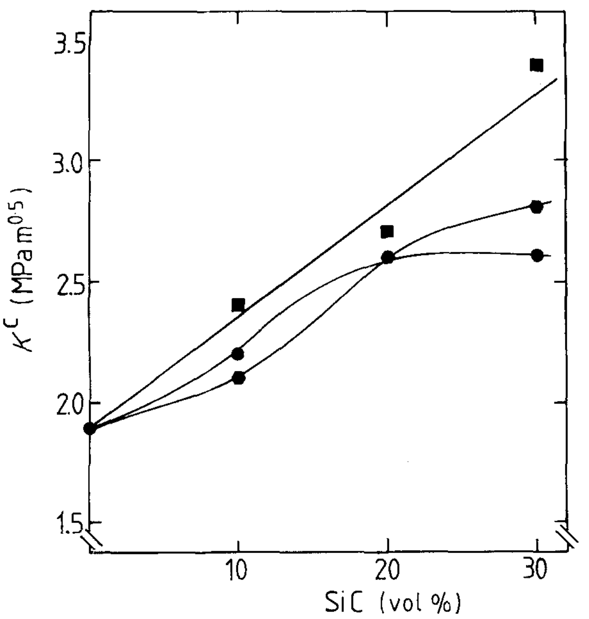

Figure 3 The fracture toughness of cordierite/silicon carbide composites as a function of SiC content. (■) Whiskers, (●) particles, (●) platelets.

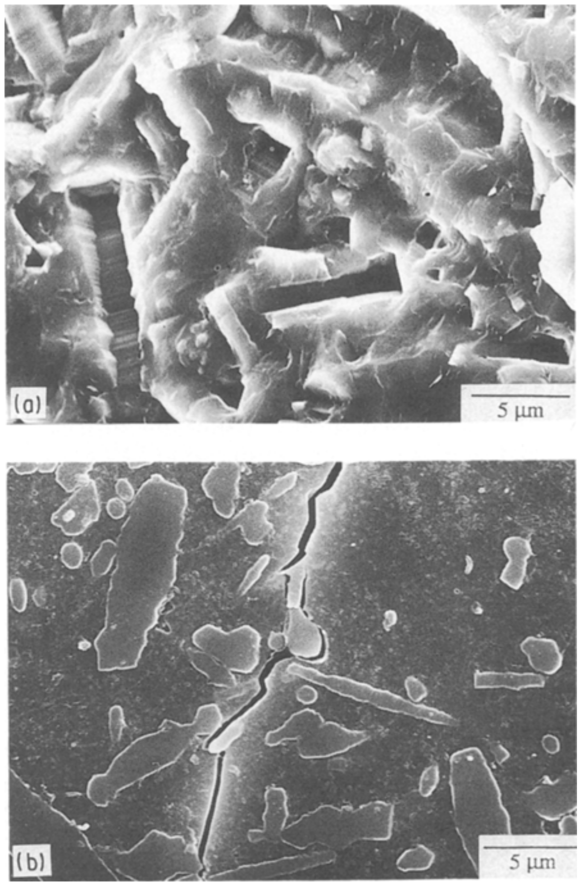

Figure 4 Scanning electron micrographs illustrating crack deflection around the SiC whiskers on (a) a fracture surface, and (b) a relief polished surface.

electron microscope (SEM) revealed that crack deflection was a major contributor to the improved fracture toughness (Fig. 4). It was observed that those whiskers lying in, or at an acute angle to, the crack plane were most effective in deflecting the crack front. Those lying orthogonal to the crack plane were generally fractured within one or two whisker diameters of the crack plane (Fig. 5). The analyses of Faber and Evans [10] indicate that, for rod-like particles, toughening due to crack deflection would reach an asymptotic value at second-phase contents approaching 20 vol %. Such behaviour was not observed for this system. It may therefore be assumed that additional toughening mechanisms contributed to the overall fracture toughness of the cordierite whisker composites.

No evidence for whisker pull-out was observed in this system under the test conditions used. In order for pull-out to occur, the whiskers must first debond from the matrix and then be drawn from their sockets against frictional forces. Such a process was not expected here for two reasons.

1. The stress distribution in a test bar subject to a bending moment is such that, if a whisker is lying at right angles to the crack plane at the point of fracture, the maximum bending stress in the whisker will occur in the crack plane. Experimental evidence of this behaviour has been presented by Campbell *et al.* [11].

2. The uneven nature of the surfaces of many of the whiskers facilitated an effective mechanical key between the whiskers and the matrix (Fig. 6). In order for pull-out to occur in such cases, the matrix would be required to fail in shear parallel to the whisker axis at the point of maximum radius (Fig. 7).

Pull-out has been used to explain the improvement in fracture toughness in whisker-reinforced ceramics, particularly in the well-studied alumina/silicon carbide whisker system [12–14]. This belief was founded on the basis that whiskers were observed to protrude

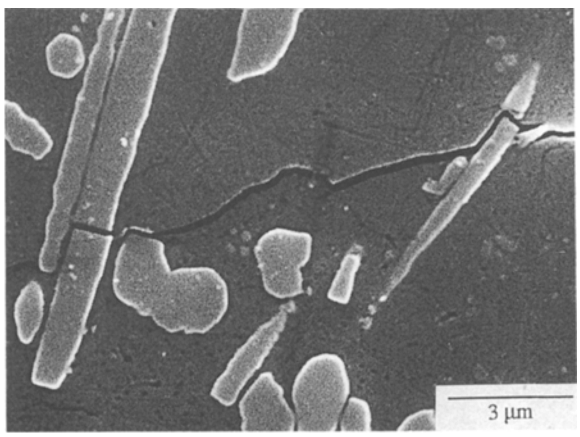

Figure 5 A scanning electron micrograph illustrating crack deflection and whisker fracture out of the matrix crack plane.

TABLE III Fracture toughness data for the composites as a function of second-phase content and morphology

Second-phase content (vol %)	Fracture toughness ($MPa^{0.5}$) Mean	S.D.
10 whiskers	2.4	0.1
20 whiskers	2.7	0.1
30 whiskers	3.4	0.1
10 particles	2.2	0.1
20 particles	2.6	0.1
30 particles	2.6	0.2
10 platelets	2.1	0.4
20 patelets	2.6	0.3
30 platelets	2.8	0.2

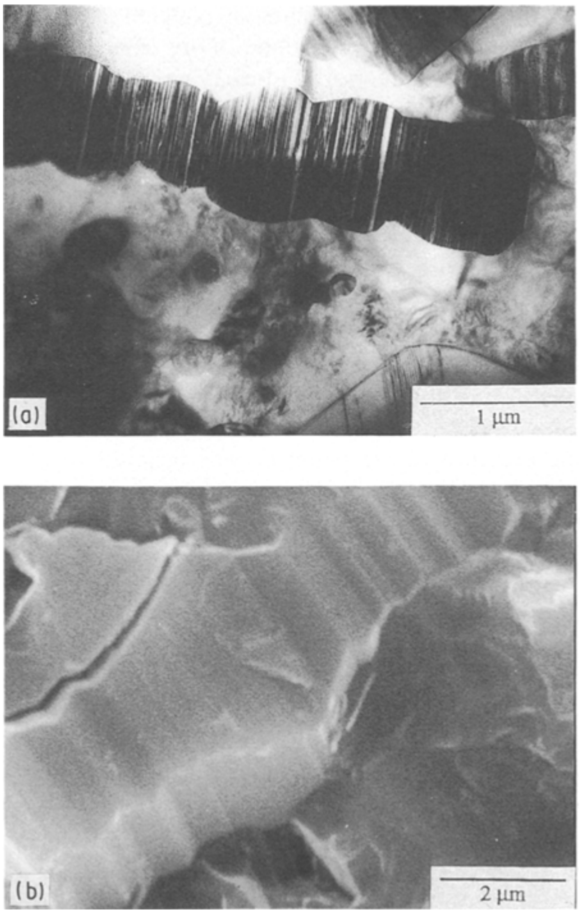

Figure 6 Effective mechanical keying of the cordierite to the surface irregularities of the whiskers. (a) Transmission electron micrograph of the interface between the matrix and a whisker. (b) Scanning electron micrograph showing fine-scale imprints produced by a SiC whisker on a fracture surface of cordierite/20 vol % SiC whiskers.

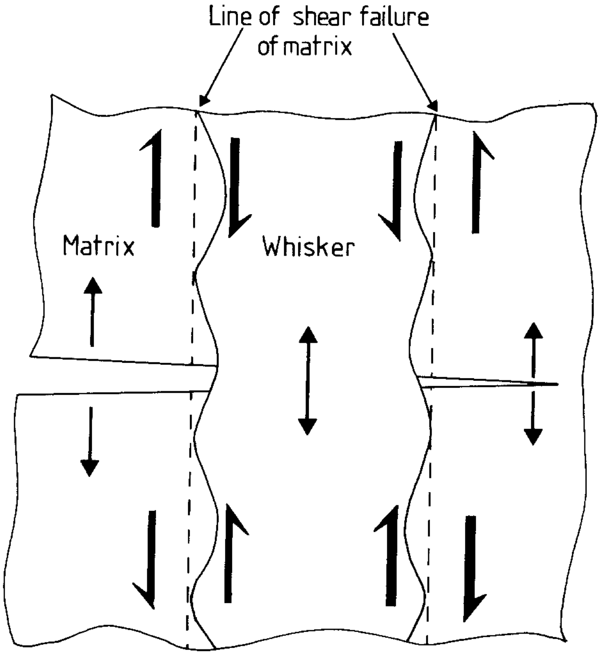

Figure 7 Schematic representation of the requirements for whisker pull-out.

above the fracture surface of the matrix. However, the lengths of the protruding ends were only of the order of twice the whisker diameter, which is small when compared to their overall length. It is suggested that

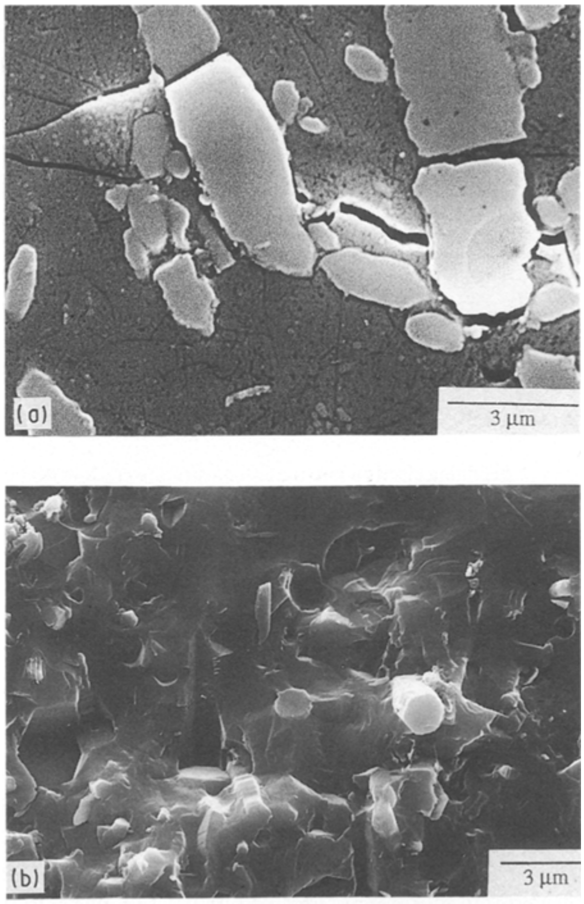

Figure 8 Scanning electron micrographs indicating the occurrence of crack bridging in (a) the near crack-tip wake of a polished section of cordierite/20 vol % SiC whiskers, and (b) sockets and protruding whisker ends on a fracture surface, indicative of the bridging process.

the process is, in fact, one of debonding, crack bridging, and whisker fracture, which has been incorrectly identified as pull-out. Becher *et al.* [15] described the process as crack bridging, where there is no requirement for sliding displacements between the whiskers and the matrix. Experimental evidence involving near crack tip studies of indentation-derived cracks suggested that this mechanism occurred in cordierite/silicon carbide whisker composites (Figs 5 and 8).

Toughening due to load transfer, may also be considered as a possible mechanism contributing to the overall fracture toughness of the composites. When loaded, the whisker and matrix strains are equivalent

$$\frac{\sigma_m}{E_m} = \frac{\sigma_f}{E_f} \quad (1)$$

where σ_m and σ_f are the matrix and fibre stresses, and E_m and E_f are the matrix and fibre elastic moduli respectively. The composite stress intensities scale with the stresses such that

$$K_c^c = \frac{K_m^c E_c}{E_m} \quad (2)$$

An improvement in fracture toughness, K, would therefore be expected by incorporating large volume fractions of high-modulus whiskers into the matrix. The contribution of this mechanism to the overall

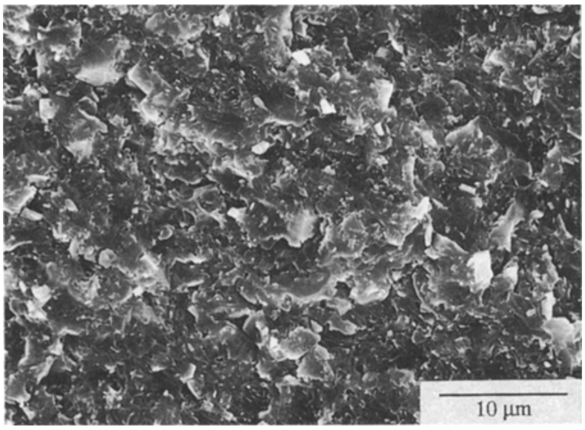

Figure 9 Scanning electron micrograph illustrating crack deflection by the SiC particles on the fracture of cordierite/20 vol % SiC.

fracture toughness of the composites cannot be accurately quantified, but the large differences in elastic moduli between the whiskers and the matrix ($E_f/E_m > 4$) would suggest that it may have a contributory effect.

The fracture toughness data for the cordierite/silicon carbide particle composites are presented in Table III and Fig. 3. Additions up to 20 vol % improved the fracture toughness of the cordierite by 37%. Further additions gave no improvement. The toughening increments derived from the particulate additions were not as substantial as those derived from the whisker additions.

In order to explain the observed differences between the whisker reinforced cordierite and the particle-reinforced cordierite, consideration should be given to the respective operative toughening mechanisms in each. The toughening of cordierite, due to whisker additions, has been explained in terms of crack deflection, crack bridging and load transfer. Crack deflection in the cordierite/particulate composites was readily observed (Fig. 9), although the perturbations of the crack front did not appear to be as severe as in the whisker-reinforced material. Crack bridging by particles of the order of 1 μm diameter was not expected because debonding of the interface would allow the crack to circumvent the particle. The contribution made by load transfer to the improved fracture toughness of the cordierite was likely to be minor and the low aspect ratio of the particles ($s = 1$) would not be expected to be sufficient to allow the build-up of significant interfacial shear stresses necessary for load transfer. If load transfer made a significant contribution to the toughness of the cordierite/particle composites, the fracture toughness would be expected to improve with increasing particle additions in excess of 10 vol %. The fact that fracture tougness reached an asymptotic value at approximately 20 vol % SiC suggests that crack deflection was the only toughening mechanism operating in this system. Hence it may be inferred that the inferior fracture toughness of the cordierite/particle composites, compared to the cordierite/whisker composites, can be attributed to the absence of crack bridging and load transfer, and to the reduction of the contribution of crack deflection.

The potential advantages of platelets over particulate reinforcement include more effective crack deflection and superior load-carrying capacity. Other possible toughening mechanisms may include crack bridging and pull-out.

Heussner and Claussen [16] incorporated alumina platelets (10 μm diameter) into yttria and ceria tetragonal zirconia polycrystals (Y-TZP and Ce-TZP). The composites were fabricated by attrition milling and hot isostatically pressing (HIPing) at 1600 °C for 1 h under a pressure of 200 MPa. They observed that, in the 2Y-TZP, their presence caused a marked reduction in fracture strength, from 1430 MPa to 736 MPa for a 5 vol % addition. The increase in flaw size, due to the presence of the platelets, was believed to be responsible. Fracture toughness, however, was marginally improved (from 8.2–9.5 $MPa\,m^{0.5}$) as a result of crack deflection and load transfer.

The mechanical behaviour of the Ce-TZP/Al_2O_3 platelet composites was somewhat different to that of the Y-TZP composites. Fracture strength was increased from 480 MPa to 520 MPa, on the addition of 10 vol % platelets. The authors believed that the improvement was due to stress redistribution by the platelets which served to increase the yield stress of the Ce-TZP. Fracture toughness, however, was reported to have been reduced on the addition of 5 vol % of platelets from 9.5–7 $MPa\,m^{0.5}$. This was explained in terms of the effect of the platelets on the transformability of the zirconia. It was believed that suppression of the autocatalytic transformation mechanism took place, thereby reducing the size of the process zone and, hence, toughness.

The fracture toughness data obtained from the cordierite/silicon carbide platelet composites is presented in Table III and Fig. 3. The nature of the curve is somewhat different from those of the whisker- and particulate-reinforced cordierite. Interpolation of the data between 0 and 10 vol % platelets indicated that little toughening would be derived from the addition of 5 vol % platelets. The explanation for this is related to the dimensions of the platelets themselves. The mean free path between the platelets in the cordierite was greater than that of either the whiskers or the particles because of their much larger dimensions.

As a consequence of the larger second-phase separation, the interaction of an indent-derived crack is dependent on the volume fraction of platelets and the location of the indentor. In general, the degree of interaction of a crack with the platelets is expected to be less than for the whiskers and particles.

The probalistic effect of the location of the indentor is highlighted in Table III. The variability of fracture toughness, presented in terms of the standard deviation in the data, indicates that a wider range of toughness values were recorded for the platelet-containing composites than for the others. Moreover, the degree of variability was most pronounced in those composites containing the lowest volume fraction of platelets. Low platelet loadings resulted in large interplatelet mean-free paths, of the order of the crack lengths. Therefore, a greater scatter in the data was observed. When platelet content was increased, the inter-platelet spacings were reduced, increasing the probability of crack interaction and reducing the scatter of the data. A further consequence of large mean-free paths was the decreased ability of the platelets to accommodate the high stress intensities generated by the large cracks. Fig. 10 indicates that fracture of the platelets took place if they were intersected by large matrix cracks.

An additional feature of interest in Fig. 10, is the nature of the cracks which have propagated left and right with respect to the micrograph. It is apparent that these cracks propagated in such a way so as to by-pass two platelets in their paths. A likely explanation for this behaviour may be the presence of large residual thermal stress fields within the matrix. The coefficient of thermal expansion of silicon carbide is $3.2\ \mathrm{m\,K^{-1}}$. The coefficient of thermal expansion of the cordierite has been measured in this work as $2.3\ \mathrm{m\,K^{-1}}$. This difference in coefficients of thermal expansion resulted in the generation of residual radial tensile stresses and circumferential compressive stresses within the cordierite, around the platelets. Owing to the large dimensions of the platelets, it is expected that these stresses would act over significant distances. A consequence of this is crack deflection occurring around the platelets, as illustrated in Fig. 10. The hypothesis above was further substantiated by the presence of secondary cracks emanating from the corners of the indentation. They were observed to propagate around the platelets, normal to the residual tensile stress axis.

For platelet additions in excess of 10 vol %, the composites exhibited a similar trend to that of the whisker and particle-reinforced materials. The data suggest that crack deflection was only one of the operative toughening mechanisms in this system. However, observations in the SEM indicated that crack deflection contributed significantly to the overall fracture toughness of these composites (Fig. 11).

No evidence of crack bridging was found, either on fracture surfaces or across indent-derived cracks. It is therefore suggested that the fracture toughness of the cordierite/platelet composites was due primarily to crack deflection, with a probable contribution from load transfer.

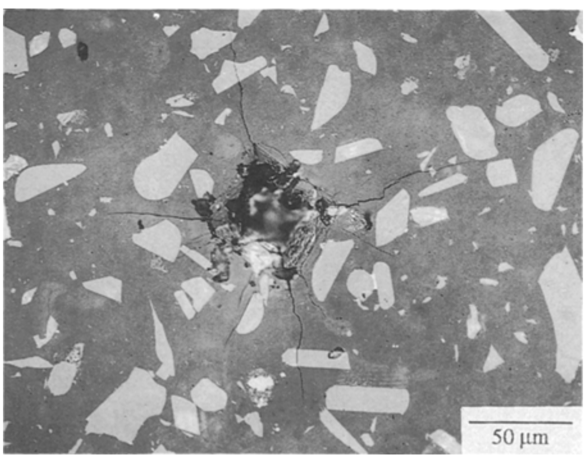

Figure 10 Optical micrograph showing the interaction of radial cracks (emanating from a Vickers indent) with SiC platelets in cordierite/30 vol % SiC platelets.

4.3. Fracture strength

The fracture strength of the composites is presented as a function of second-phase content in Table IV and Fig. 12. During loading, all composites exhibited Hookean behaviour with no evidence of non-linearity prior to catastrophic failure. Some evidence of non-linearity has, however, been reported in silicon carbide whisker-reinforced alumina ceramics [14, 17]. Jenkins *et al.* [17] observed crack arrest in Chevron-notched specimens and explained the behaviour in terms of

TABLE IV Fracture strength data for the composites as a function of second-phase morphology and content

Second-phase content (vol %)	Fracture strength (MPa) Mean	S.D.
10 whiskers	190	20.1
20 whiskers	220	25.4
30 whiskers	241	26.8
10 particles	200	13.2
20 particles	248	14.5
30 particles	275	16.5
10 platelets	136	6.0
20 platelets	139	6.6
30 platelets	144	6.4

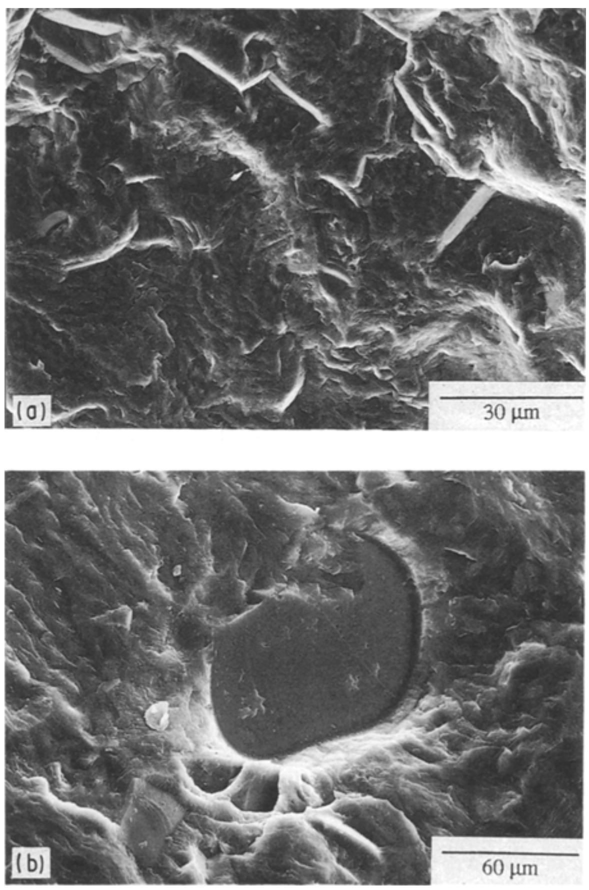

Figure 11 Scanning electron micrographs indicating significant crack deflection in cordierite/SiC platelet composites. (a) Large tilt and twist and twist angles, and (b) an impression left by a platelet circumvented by the propagating crack.

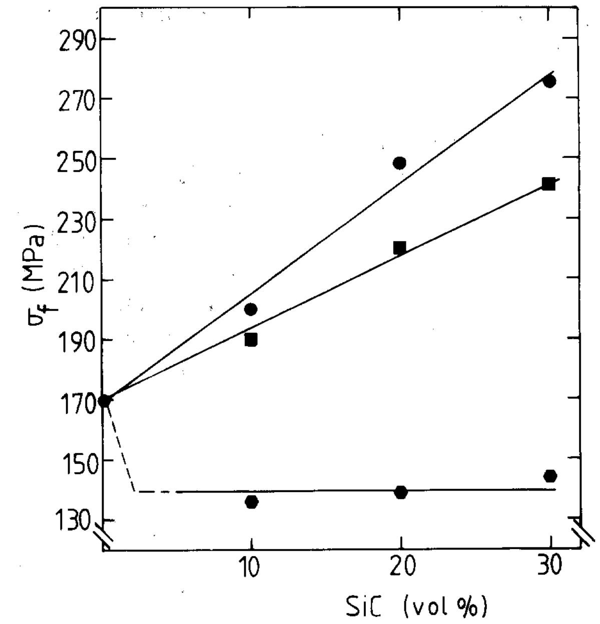

Figure 12 Fracture strength of cordierite/SiC composites as a function of SiC content. (■) Whiskers, (●) particles, (●) platelets.

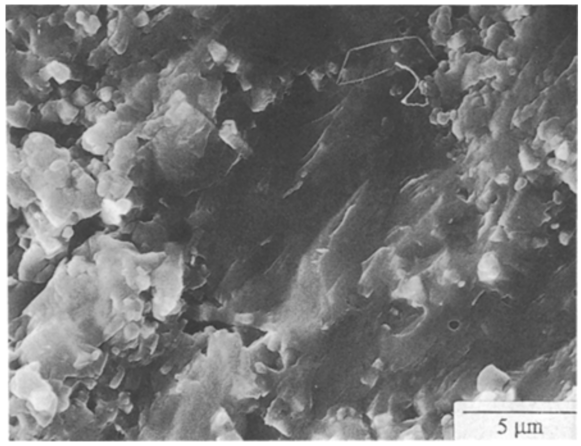

Figure 13 Scanning electron micrograph illustrating a whisker-derived flaw network in cordierite/30 vol % SiC whiskers.

TABLE V Calculated critical flaw size in the cordierite/silicon carbide composites

Second-phase content (vol %)	Critical flaw size (μm)
10 whiskers	40
20 whiskers	38
30 whiskers	51
10 particles	31
20 particles	28
30 particles	23
10 platelets	61
20 platelets	89
30 platelets	96

whisker bridging in the crack wake. Shalek *et al.* [4] reported a degree of non-linearity in the load–deflection curves of silicon carbide whisker-reinforced silicon nitride. They believed that micro-crack process zones were responsible. Similar observations were made by Gac *et al.* [18], in silicon carbide whisker-reinforced borosilicate glass. The fracture strength of the whisker-reinforced cordierite exhibited a linear dependence on whisker content over the range of compositions studied, despite the associated increase in critical flaw size (Table V).

Fractographic studies by scanning electron microscopy enabled the cause of the increased flaw size to be established (Fig. 13). The micrograph indicated a flaw associated with the whisker networks. The fracture strength data illustrate that the beneficial effects of an improved fracture toughness and load transfer by the whiskers predominated over the detrimental effect of an increased flaw size.

Addition of the particulate silicon carbide to the cordierite matrix resulted in a marked improvement in fracture strength with the strengthening increment greater than for the equivalent whisker-reinforced material (Fig. 12). As in the case of the whisker-reinforced cordierite, an improvement in fracture strength might well have been predicted from the fracture toughness data. On this basis alone, it would be expected that the fracture strength of the particulate-reinforced cordierite would be inferior to that of the material reinforced by whiskers. The apparent discrepancy is compounded by the fact that strengthening due to load transfer would not be expected to take place in the particulate composites. An explanation for the results lies in the effect of the particles on the apparent flaw size of the material. Unlike the whisker-reinforced cordierite, particulate additions brought about a reduction in flaw size (Table V). In such cases, the second phase interacts with the inherent matrix flaws, thereby reducing their effective size. Hasselman and Fulrath [19] have demonstrated that if the mean particle spacing is greater than the critical flaw size of the matrix, then only marginal improvements in fracture strength may be achieved. Once the particle content exceeds a critical value, corresponding to a mean spacing equivalent to the matrix flaw size, then significant improvments in fracture strength may be achieved. The mean-free path, R, between randomly distributed monosized particles may be estimated from the following equation derived by Fullman [20]

$$R = \frac{4d(1 - V_p)}{3V_p} \qquad (3)$$

where d is the particle diameter, and V_p the volume fraction of particles. Although Equation 3 applies to monosized particles, it may be used as an approximation for non-ideal systems. The calculated mean-free paths for the SiC particle-reinforced cordierite is presented in Table VI. A value of 1 μm was used for the mean particle size. The estimated values are lower than the calculated critical flaw sizes of the composites because they represent mean values. However, the fracture process initiates from the largest flaw which is favourably orientated; that is to say, the one which experiences the maximum stress intensity at its tip. The data appear to be consistent in that they are of the same order and exhibit a downward trend with increasing particle content.

TABLE VI The calculated mean path in cordierite/SiC particulate composites, as a function of particle content

SiC content (vol %)	R (μm)
10	12.0
20	5.3
30	3.1

The addition of silicon carbide platelets to cordierite had a detrimental effect on fracture strength, over the range of compositions studied (Fig. 12 and Table IV). Moreover, the fracture strength was not observed to vary as a function of platelet content.

The addition of 10 vol % platelets reduced the fracture strength of the cordierite from 170 MPa to 136 MPa. Similar values were recorded for those composites containing 20 and 30 vol % platelets. The fracture behaviour of the cordierite/platelet composites was quite different to that of the whisker- and particle-reinforced materials. The difference was not related to the morphology of the platelets, but to their dimensions. The fracture surfaces illustrated in Fig. 11 demonstrate that interfacial fracture was commonplace, suggesting that no interfacial bonding had taken place during fabrication.

The fracture behaviour may be explained in terms of the effect of the platelets on the flaw size of the composites (Table V). The calculated critical flaw size is comparable to the dimensions of the largest platelets present. These data indicate that the flaw size increased with increasing platelet content. Three possible reasons can account for this: (1) the formation of agglomerates; (2) the presence of larger particles; (3) the increasing overlap of stress fields associated with the platelets. The first possibility exploits the argument that, as the second-phase content is increased, dispersion becomes progressively more difficult. No such observations were made in the cordierite/silicon carbide platelet composites. It is believed that platelet agglomeration did not occur due to their large dimensions, rendering the effect of Van der Waals attractive forces negligible and, thus, permitting their easy dispersion.

The second possibility is that, as the platelet content is increased, there may be an increased probability of larger platelets being present. Such an occurrence would manifest itself in the degree of scatter in the fracture data (Table IV). This was clearly not the case.

The final possibility may be due to the overlap in the stress fields around the platelets when the composites were stressed. Although the dimensions of the second phase do not affect the magnitude of the residual stresses generated, they do affect the distance over which the stresses operate [21]. It therefore seems probable that an increase in the platelet content will increase the overlap in the stress fields and thus increase the apparent flaw size of the composites.

4. Summary

A study of the fabrication and mechanical properties of cordierite composites containing silicon carbide of different morphologies has been carried out. Several conclusions may be drawn.

1. Composites containing whiskers required the most severe conditions to obtain densities approaching the theoretical values. It is suggested that this was due to the formation of rigid contiguous networks of whiskers, which severely retarded the densification process.

2. The maximum toughening increment was derived from the addition of whiskers. It has been established that the mechanisms of crack deflection and crack bridging contributed to the improved fracture toughness over the unreinforced cordierite. It is suggested that a contribution may have also been made by the load-transfer mechanism, due to the significant differences in elastic moduli between the whiskers and matrix. However, no evidence of whisker pull-out was observed.

For second-phase contents in excess of 20 vol %, the platelets proved to be more effective in toughening the cordierite than did the particulate silicon carbide. This is believed to have been due to a greater contribution from the crack deflection mechanism, coupled with a possible contribution from load transfer, which was believed to be absent in the particle-containing composites. For composites containing 20 vol % platelets or less, the recorded toughness values are questionable, because the degree of crack interaction with the platelets was limited and dependent on the precise location of the indentor on the sample surface. In many cases cracks were observed to propagate through the matrix without interacting with any platelets. This phenomenon is manifest in the degree of scatter in the fracture toughness data. The large dimensions of the platelets were responsible for the infrequency with which indentation-derived cracks interacted with the second phase.

3. The fracture strength of those composites containing particulate silicon carbide were superior to the equivalent platelet and whisker-containing composites despite their inferior fracture toughness. The strengthening effects of a reduction in critical flaw size with increasing particle additions, augmented the increase due to an improved fracture toughness.

The inferior fracture strength of the whisker-containing composites, when compared to those containing particulate silicon carbide, was due to the fact that the whiskers increased the critical flaw size of the composites. It has been established that this was due to the formation of flaws associated with the whisker network structure. The beneficial effects of superior fracture toughness on fracture strength were insufficient to compensate for the detrimental effects caused by an increase in flaw size.

The fracture strength data for the cordierite/silicon carbide platelet composites are apparently anomalous in that the platelets have a weakening effect. It has been established that this was due to the occurrence of flaws associated with the matrix–platelet interface, which were larger than the inherent matrix flaws.

4. A direct comparison between the whisker- and particle-reinforced cordierite composite properties was possible, but the platelet dimensions were an

order of magnitude greater, preventing such comparisons being meaningful. Clearly, finer platelets are required, becuase they would be more effective in toughening the cordierite matrix, particularly at low concentrations. It is also expected that fracture strength would be improved due to a reduction in flaw size of the composites. However, it is predicted that the fracture toughness of such composites will still be inferior to those containing whiskers. Therefore, if maximum toughness is required, whisker reinforcement should be used, but this needs to be considered in conjunction with the particular problems associated with handling, fabricating and using such composites.

5. Conclusions

1. The addition of silicon carbide, particularly in the form of whiskers, had an adverse effect on the ease of densification of the cordierite matrix.

2. The fracture toughness of the composites was dependent on the morphology, dimensions and volume fraction of the silicon carbide used. However, in all cases the fracture toughness was superior to the unreinforced cordierite. The most significant improvements were derived from whisker additions, than from platelets with the least significant improvements being recorded in those composites containing silicon carbide particles.

3. The fracture strengths of the composites were governed by the relative contributions from an increase in fracture toughness and the change in critical flaw size associated with the presence of the second phase. In those composites containing silicon carbide whiskers and particles, fracture strength was improved significantly, whereas silicon carbide platelets had an adverse effect on fracture strength.

References

1. J. D. BIRCHALL, D. R. STANLEY, M. J. MOCKFORD, G. H. PIGOTT and P. J. PINTO, *J. Mat. Sci. Lett.* **6** (1988) 350.
2. M. F. STANTON, M. LEYARD, A. TEGERIS, E. MILLER, M. MAY, E. MORGAN and A. SMITH, *J. Nat. Cancer Inst.* **67** (1981) 965.
3. M. CHAMBERLAIN, R. DAVIES, R. C. BROWN and D. M. GRIFFITHS, in '*In Vitro* Tests For The Pathogenicity Of Mineral Dusts In Inhaled Particles', edited by W. H. Walton (Pergamon Press, Oxford, 1982) p. 583.
4. P. D. SHALEK, J. J. PETROVIC, G. F. HURLEY and F. D. GAC, *Amer. Ceram. Soc. Bull.* **65** (1986) 351.
5. W. BRAUE, A. HOLISHER, B. SARUHAN, and G. ZIEGLER, in "Proceedings of the First European Ceramic Society Conference", Vol. 3, Maastricht, The Netherlands, 18–23 June 1989, edited by G. de With, (Elsevier, UK) p. 263.
6. A. G. EVANS and E. A. CHARLES, *J. Amer. Ceram. Soc.* **59** (1976) 371.
7. G. R. ANSTIS, P. CHANTIKUL, B. LAWN and D. B. MARSHALL, *ibid.* **64** (1981) 533.
8. P. CHANTIKUL, G. R. ANSTIS, B. R. LAWN and D. B. MARSHALL, *ibid.* **64** (1981) 539.
9. W-H. TUAN, PhD thesis, Leeds University (1988).
10. K. T. FABER and A. G. EVANS, *Acta. Metall.* **31** (1983) 565.
11. G. H. CAMPBELL, M. RUHLE, B. J. DALGLEISH and A. G. EVANS, *J. Amer. Ceram. Soc.* **73** (1990) 521.
12. G. C. WEI and P. F. BECHER, *ibid.* **67** (1984) C-267.
13. P. F. BECHER and G. C. WEI, *Amer. Ceram. Soc. Bull.* **64** (1985) 298.
14. M. YANG, PhD thesis, Leeds University (1988).
15. P. F. BECHER, C-H. HSEUH, P. ANGELINI and T. N. TIEGS, *J. Amer Ceram. Soc.* **71** (1988) 1050.
16. K. H. HEUSSNER and N. CLAUSSEN, *J. Euro. Ceram. Soc.* **5** (1989) 193.
17. M. G. JENKINS, A. S. KOBAYASHI, K. W. WHITE and R. C. BRADT, *J. Amer. Ceram. Soc.* **70** (1987) 393.
18. F. D. GAC, J. J. PETROVIC, J. V. MILEWSKI and P. D. SHALEK, *Ceram. Engng Sci. Proc.* **7** (1986) 978.
19. D. P. H. HASSELMAN and R. M. FULRATH, *J. Amer. Ceram. Soc.* **49** (1966) 68.
20. R. L. FULLMAN, *Trans. Amer. Inst. Metals* **197** (1953) 47.
21. J. SELSING, *J. Amer. Ceram. Soc.* **44** (1961) 419.

Received 12 March
and accepted 20 March 1991